Upregulation of the *N*-Formyl Peptide Receptors in Scleroderma Fibroblasts Fosters the Switch to Myofibroblasts

Francesca Wanda Rossi,* Filomena Napolitano,* Ada Pesapane,* Massimo Mascolo,† Stefania Staibano,† Marco Matucci-Cerinic,‡ Serena Guiducci,‡ Pia Ragno,§ Gaetano di Spigna,* Loredana Postiglione,* Gianni Marone,* Nunzia Montuori,* and Amato de Paulis*

Systemic sclerosis (SSc) is characterized by chronic inflammation and fibrosis. *N*-Formyl peptide (fMLF) receptors (FPRs) are chemotactic receptors involved in inflammation. Three FPRs have been identified: FPR1, FPR2, and FPR3. We have examined, by RT-PCR, Western blot and immunohistochemistry, FPRs expression in skin fibroblasts from 10 normal subjects and 10 SSc patients, showing increased expression in SSc fibroblasts. Several functions of FPRs occur through the interaction with a region of the urokinase-type plasminogen activator receptor ($uPAR_{88–92}$), able to interact with FPRs and to mediate urokinase (uPA) or fMLF-dependent cell migration. Soluble $uPAR_{84–95}$ peptide can act as a direct ligand of FPRs. Furthermore, uPA or its amino-terminal fragment (ATF) can promote the exposure of the $uPAR_{88–92}$ region. The WKYMVm peptide is a FPRs pan-agonist. We investigated the functional effects of these agonists on normal and SSc fibroblasts. ATF, $uPAR_{84–95}$, and WKYMVm regulated adhesion, migration, and proliferation of normal fibroblasts. Despite FPR overexpression, the response of SSc fibroblasts to the same agonists was greatly reduced, except for the proliferative response to ATF. SSc fibroblasts showed increased α-smooth muscle actin expression and improved capability to induce wound closure. Indeed, they overexpressed a cleaved uPAR form, exposing the $uPAR_{88–92}$ region, and vitronectin, both involved in fibrosis and in the fibroblast-to-myofibroblast transition. FPR stimulation promoted α-smooth muscle actin expression in normal fibroblasts as well as motility, matrix deposition, $\alpha_v\beta_5$ integrin expression, and radical oxygen species generation in normal and SSc fibroblasts. This study provides evidence that FPRs may play a role in fibrosis and in the fibroblast-to-myofibroblast transition. ***The Journal of Immunology*****, 2015, 194: 5161–5173.**

Systemic sclerosis (SSc) is a chronic systemic disease characterized by impaired communication between endothelial cells, epithelial cells and fibroblasts, lymphocyte activation, autoantibody production, inflammation, and connective tissue fibrosis (1). The pathogenesis of SSc is extremely complex. and despite a number of studies that examined several aspects of its intricate picture, the mechanisms involved are still largely unknown. During the past decade, considerable attention has been paid to the origin of myofibroblast, the mesenchymal cell type most responsible for the excessive matrix production and deposition in tissue and vessel wall, found in fibrotic disorders and fibroproliferative vasculopathies (2). However, in SSc, the origin of myofibroblasts has not been completely elucidated (3). In fibrotic diseases, myofibroblasts may derive from at least three sources: 1) expansion and activation of resident tissue fibroblasts; 2) transition of epithelial cells into mesenchymal cells, a process known as epithelial–mesenchymal transition; and 3) tissue migration of bone marrow–derived circulating fibrocytes (4). Under normal circumstances, the fibroblast repair program is self limited, but pathological fibrotic responses are characterized by sustained and amplified fibroblast activation (5).

In SSc, inappropriate fibroblast activation and subsequent accumulation of myofibroblasts in affected tissues and the persistence of their elevated biosynthetic functions are crucial determinants of the extent and rate of fibrosis and influence significantly also the clinical course of the disease as well as the response to therapy, thus dictating the prognosis and the overall mortality (6). Recently, endothelial mesenchymal transition (EndoMT), a newly recognized type of cellular transdifferentiation, has emerged as another possible source of tissue myofibroblasts, deeply involved in the pathogenesis of fibrotic diseases (7).

EndoMT is a complex biological process in which endothelial cells lose their specific endothelial cell markers, such as vascular endothelial cadherin. Consequently, fibroblasts acquire a mesenchymal or myofibroblast phenotype, expressing its typical markers, such as α-smooth muscle actin (α-SMA), vimentin, and types I and III interstitial collagens. Besides the acquisition of an activated profibrogenic phenotype, these cells also become motile and capable of migrating into surrounding tissues (8). Today, the EndoMT process is gaining increased attention in fibrotic disorders, although only few experimental evidences support the participation of EndoMT in the pathogenesis of SSc (8).

*Department of Translational Medical Sciences and Center for Basic and Clinical Immunology Research, University of Naples Federico II, 80131 Naples, Italy; †Department of Advanced Biomedical Sciences, University of Naples Federico II, 80131 Naples, Italy; ‡Department of Biomedicine, University of Florence, 50121 Florence, Italy; and §Department of Chemistry and Biology, University of Salerno, 84084 Salerno, Italy

Received for publication November 6, 2014. Accepted for publication March 30, 2015.

This work was supported in part by grants from the Compagnia di San Paolo and Polo delle Scienze e delle Tecnologie per la Vita (Progetto F.A.R.O. 2012), as well as Regione Campania Center for Basic and Clinical Immunology Research-Lab, CRÈME and TIMING projects and Campania Bioscience Grant PON03PE_0060_08.

Address correspondence to Prof. Nunzia Montuori, Department of Translational Medical Sciences and Center for Basic and Clinical Immunology Research, University of Naples Federico II, Via Pansini 5, 80131 Naples, Italy. E-mail address: nmontuor@unina.it

Abbreviations used in this article: ATF, aminoterminal fragment; DCHF-DA, 2′,7′-dichlorodihydrofluorescein diacetate; ECM, extracellular matrix; EndoMT, endothelial mesenchymal transition; FPR, formyl-peptide receptor; ROS, radical oxygen species; α-SMA, α smooth muscle actin; SSc, systemic sclerosis; uPA, urokinase-type plasminogen activator; uPAR, uPA receptor.

Moreover, the origin of myofibroblasts in SSc may also include pericyte cells (9). Small blood vessels make up two cell types: endothelial cells and pericytes. Microvascular pericytes are in intimate contact with, and modulate the function of, endothelial cells. In SSc, such pericytes may contribute to the overproduction of extracellular matrix (ECM) molecules and constitute a cellular link between microvascular damage and fibrosis by transdifferentiating into myofibroblasts (10).

The *N*-formyl peptide receptor (FPR) family is a group of cell surface receptors acting as pattern recognition receptors, regulating many cellular activities, such as migration, proliferation, differentiation, growth, and death. Their involvement in innate inflammatory responses is well established (11). Three FPRs have been identified in humans, namely FPR1, FPR2, and FPR3 (12). FPRs, by interacting with several structurally diverse pro- and anti-inflammatory ligands, seem to possess important regulatory effects in multiple pathological conditions, including inflammation, amyloidosis, Alzheimer's disease, prion disease, AIDS, obesity, diabetes, and cancer (13). FPR1 is activated by nanomolar concentrations of fMet-Leu-Phe (fMLF), a potent leukocyte chemoattractant (11). FPR2 is a promiscuous receptor activated in response to high concentration of fMLF, viral, bacterial, endogenous, and synthetic peptides (12). Hp(2–20) (14), and F2L (15) are natural ligands for FPR3. The synthetic peptide WKYMVm (11) is an FPR panagonist. All FRRs expressed on epithelia seem to be required for wound repair and restitution of barrier integrity. In this regard, we have recently demonstrated that FPRs activation facilitates epithelial cell migration, proliferation, and neoangiogenesis in gastric and nasal epithelial cells (16, 17).

One regulator of the signal transduction pathways, involved in both epithelial mesenchymal transition (18) and EndoMT (19), is the urokinase-type plasminogen activator (uPA)–uPA receptor (uPAR) system. uPAR is formed by three homologous domains (DI, DII, and DIII) anchored to the cell surface by a GPI tail (20). The main uPAR activity is the focusing of proteolytic uPA activity on the cell membrane (21). uPA is a serine protease that activates plasminogen to plasmin; uPA or its aminoterminal fragment (ATF), devoid of enzymatic activity, binds uPAR with high specificity and affinity (22). However, uPAR has also been reported to be a major protein involved in other events such as wound repair, tumor progression, angiogenesis, by interacting with integrins, FPRs, and tyrosine kinase receptors (23).

In addition, uPAR binds vitronectin, which has been reported to be an extracellular matrix protein that develops in response to tissue injury, especially in the early provisional matrix (24) involved in liver and lung disease, where its expression is closely associated with fibrosis (25). Vitronectin, also known as S protein of the complement regulatory pathway, has been demonstrated by in vitro studies to bind cellular receptors including the integrins $\alpha_v\beta_3$ and $\alpha_v\beta_5$, which are also uPAR coreceptors (18).

FPR interaction with uPAR mediates uPA-dependent cell migration and is required for chemotaxis induced by fMLF (26). A specific site corresponding to aa 88–92 (SRSRY), located in the flexible linker connecting the uPAR domains DI and DII, is responsible of uPAR cross-talk with FPRs (27). In fact, the soluble $uPAR_{84–95}$ peptide can promote directional cell migration by binding to FPRs, thus representing an endogenous ligand of FPRs (27). Exposure of $uPAR_{84–92}$ region on the cell membrane is favored by uPAR cleavage (26) or by uPA binding to uPAR (28).

Previously, we focused our attention on the urokinase-mediated plasminogen activation (PA) system in skin fibroblasts of SSc, highlighting a role of uPA and uPAR in the disease (29). Furthermore, it has been demonstrated that, in SSc, uPAR represents a critical effector molecule also in endothelial cells, contributing to their migration and differentiation. Indeed, in microvascular endothelial cells of diffuse SSc, uPAR cleavage operated by overexpressed matrix metalloproteinase-12 contributes to the impaired angiogenesis observed both in vitro and in SSc patients (30).

To test the possibility that fibroblast FPRs are involved in the pathogenesis of SSc and that uPAR–FPR interaction may be crucial, in particular, in the fibroblast-to-myofibroblast transition, we investigated whether FPRs are expressed on human skin fibroblasts of patients affected by different grade of SSc and whether their activation plays a role in some as yet unexplained mechanisms involved in SSc, such as wound healing, tissue remodeling, and fibrosis.

To our knowledge, we provide, for the first time, evidence of FPR overexpression in human skin SSc fibroblasts, both in vivo and in vitro. We also show that their activation through specific agonists may contribute to a myofibroblast phenotype of SSc fibroblasts because FPRs stimulation is able to increase α-SMA expression in normal skin fibroblasts as well as $\alpha_v\beta_5$ integrin expression, ECM deposition, and reactive oxygen species (ROS) production in both normal and SSc fibroblasts. Taken together, all our observations emphasize the intriguing role of these receptors in the pathogenesis of SSc.

Materials and Methods

Peptides and chemicals

The hexapeptide Trp-Lys-Tyr-Met-Val-D-Met-NH2 (WKYMVm) was synthesized and HPLC purified (>95%) by Innovagen (Lund, Sweden), the peptide $uPAR_{88–92}$ was synthesized by PRIMM (Milan, Italy), and the uPA N-terminal fragment (ATF-uPA) was from American Diagnostica (Greenwich, CT).

TRIzol solution was from Invitrogen Fischer Scientific (Illkirch, France), and DNA ladder and Moloney leukemia virus reverse transcriptase were from Promega (Madison, WI). Protein concentration was estimated with a modified Bradford assay (Bio-Rad Laboratories). CellTiter 96 Aqueous One Solution Reagent was from Calbiochem (San Diego, CA), ECL Plus was from GE Healthcare (Buckinghamshire, UK), and 2′,7′-dichlorodihydrofluorescein diacetate (DCHF-DA) was from Molecular Probes (Invitrogen, Paisley, UK).

The mixture of protease and phosphatase inhibitors was from Calbiochem. Mouse anti-FPR1, rabbit anti-FPR2, mouse anti-FPR3, rabbit anti-$\alpha_v\beta_5$ integrin, mouse anti-collagen type I, and mouse anti-fibronectin were from Santa Cruz Biotechnology (Santa Cruz, CA), rabbit anti-FPR2 for immunocytochemistry mouse anti–α-SMA, mouse anti-tubulin, and rabbit anti-actin were from Sigma-Aldrich (St. Louis, MO), mouse anti-vitronectin was from Chemicon International (Temecula, CA), mouse anti-$uPAR_{84–95}$ was from PRIMM. Secondary anti-mouse and anti-rabbit Abs coupled to HRP were from Bio-Rad (Munchen, Germany). For chemotaxis assay 8-μm-pore polycarbonate membranes (Nucleopore, Pleasanton, CA) coated with 10 μg/ml fibronectin (Roche, Mannheim, Germany) were used. Fibronectin (Roche), collagen type I (Chemicon International), or vitronectin (BD Biosciences, Bedford, MA) were used for plastic coating.

Tissues and patients samples

Eight females and two males affected, observed from January 2011 to December 2013 in the Day Hospital of the Department of Translational Medical Sciences of the University of Naples Federico II, were classified according to the American College of Rheumatology criteria (31) as having limited cutaneous SSc ($n = 6$) or diffuse cutaneous (dcSSc; $n = 4$) (32) and included in the study. All patients signed a written informed consent according to the guidelines of the institutional review board for the use of humans in research. The mean age of patients was 54 y (range, 31–70 y). Disease duration was calculated from the time of onset of the first clinical event (other than Raynaud's phenomenon) that was a clear manifestation of SSc. Patients were classified as having an early-stage ($n = 4$) or late-stage ($n = 6$) SSc, according to disease duration (<5 y for early-stage limited cutaneous SSc and <3 y for early-stage diffuse cutaneous SSc) and skin histopathology (33). We considered clinically involved skin for values of skin thickness ≥ 2, according to the modified Rodnan skin thickness score. All patients with the diffuse form had involvement of

dorsal arm and/or thorax. To reduce variability among the patients, we admitted for study only SSc patients positive for antinuclear Abs, showing a speckled pattern as evaluated by indirect immunofluorescence and ELISA. Because antinuclear Ab positivity may be considered not sufficient for subtype characterization, other clinical measures were investigated; in particular, all patients with diffuse cutaneous SSc presented anti–SCL-70 topoisomerase I positivity, and patients with limited cutaneous SSc showed serum anticentromere (CENP-B) positivity. All patients were washed out from steroid treatment 30 d before the biopsy was taken. Other treatments were allowed (proton pump inhibitors, vasodilators, and so on). Patients who could not undergo washout because of the severe organ complications were not evaluated. Patients with symptoms overlapping with those of other autoimmune, rheumatic, and/or connective tissue diseases were excluded from the study. Control donors were matched with each scleroderma patient for age, sex, and biopsy site, and control samples were processed in parallel control (eight females and two males; mean ± SD age, 43 ± 15 y).

Cell culture

Surgical fragments were mechanically dissociated under a light microscope and subjected to trypsinization for 30 min at 37°C, as described previously (29). After two PBS washings, cells were plated and cultured in monolayer in DMEM (Life Technologies Carlsbad, CA) supplemented with 10% heat-inactivated FBS (Life Technologies), 100 U/ml penicillin G sodium, and 100 μg/ml streptomycin sulfate, at 37°C, in a humidified atmosphere of 5% CO_2. Fibroblasts from normal subjects and from patients with SSc were used between the 3rd and 10th passage in culture. The KG-1 (juman myeloid cell line), the K-562 (human myelogenous leukemia cell line), and the U-937 (human leukemic monocyte lymphoma cell line) were grown in RPMI 1640 medium (Life Technologies) supplemented with 10% FBS. The BJ (human foreskin fibroblasts) were grown in DMEM (Life Technologies) supplemented with 10% FBS.

RNA purification and analysis

Total cellular RNA was isolated by lysing cells in TRIzol solution, according to the supplier's protocol (28). RNA was precipitated and quantitated by spectroscopy. Five micrograms of total RNA was reversely transcribed with random hexamer primers and 200 U murine Moloney leukemia virus reverse transcriptase. One microliter of reverse-transcribed DNA was then amplified for FPR1, FPR2, FPR3, and GAPDH using specific primers. The primers for FPR1 were 5′-ATGGAGACAAATTCCTCTCTC (sense) and 3′-CACCTCTGCAGAAGGTAAAGT (antisense) (26); for FPR2 were 5′-CTTGTGATCTGGGTGGCTGGA (sense) and 3′-CATTGCCTGTAACTCAGTCTC (antisense) (28); and for FPR3 were 5′-AGTTGCTCCACAGGAATCCA (sense) and 3′-GCCAATATTGAAGTGGAGGATCAGA (antisense) (34). The primers for GAPDH were 5′-GCCAAAGGGTCATCATCTC (sense) and 3′-GTAGAGGCAGGGATGATGTTC (antisense). PCR products, together with a DNA ladder as a size standard, were separated on a 1% agarose gel, stained with ethidium bromide, and quantified with the image analysis system ChemiDoc XRSn (Bio-Rad Laboratories).

Western blot analysis

Immunoblotting experiments were performed according to standard procedures (28). Briefly, cells were harvested in lysis buffer (50 mM HEPES, 150 mM NaCl, 10% glycerol, 1% Triton X-100, 1 mM EGTA, 1.5 mM $MgCl_2$, 10 mM NaF, 10 mM sodium pyrophosphate, and 1 mM Na_3VO_4) supplemented with a mixture of proteases and phosphatases inhibitors. Fifty micrograms of protein was electrophoresed on a 10% SDS-PAGE and transferred onto a polyvinylidene fluoride membrane. The membrane was blocked with 5% nonfat dry milk and probed with specific Abs: mouse anti-FPR1 (1 μg/ml), rabbit anti-FPR2 (1 μg/ml), mouse anti-FPR3 (1 μg/ml), mouse anti–α-SMA (2 μg/ml), mouse anti-vitronectin (1 μg/ml), mouse anti-uPAR84–95 (1 μg/ml), rabbit anti-$\alpha_v\beta_5$ integrin (1 μg/ml), mouse anti-tubulin (0.5 μg/ml), and rabbit anti-actin (0.5 μg/ml). Finally, washed filters were incubated with HRP-conjugated anti-rabbit or anti-mouse Abs. The immunoreactive bands were detected by a chemiluminescence kit and quantified by densitometry (ChemiDoc XRS, Bio-Rad).

Cell adhesion assay

The adhesion assays were conducted in 96-well flat-bottom plates for cell (Nunc). Wells were coated with 1 μg collagen type I or with 100 ml heat-inactivated 1% BSA in PBS, as a negative control, and incubated overnight at 4°C. The plates were then blocked 1 h at room temperature with 1% heat-inactivated 1% BSA in PBS. Cells were detached with PBS containing 2 mM EDTA and then washed with serum-free DMEM, counted, distributed into the wells at a density of 10^5 cells/well, and incubated for 1 h at 37°C in the presence or in the absence of ATF-uPA (10^{-8} M), $uPAR_{84–95}$ (10^{-9} M), and WKYMVm peptide (10^{-9} M). Attached cells were fixed with 3% paraformaldehyde in PBS for 10 min and then incubated with 2% methanol for 10 min. Cells were finally stained for 10 min with 0.5% crystal violet in 20% methanol. Stain was eluted by 0.1 mol/l sodium citrate in 50% ethanol (pH 4.2), and the absorbance at 540 nm was measured by a spectrophotometer.

Chemotaxis assay

Human skin fibroblasts chemotaxis was performed using a modified Boyden chamber technique (35). Briefly, 25 μl of medium alone or added with chemoattractants (ATF-uPA [10^{-8} M], $uPAR_{84–95}$ [10^{-9} M], and WKYMVm peptide (10^{-9} M)] were placed in triplicate in the lower compartment of a 96-well microchemotaxis chamber (NeuroProbe, Cabin John, MD). The lower compartments were covered with 8-μm-pore polycarbonate membranes coated with 10 μg/ml fibronectin. Fifty microliters of the cell suspension (5×10^4/well), resuspended in medium alone, was loaded into the upper compartments. The chemotactic chamber was then incubated for 6 h at 37°C in a humidified incubator with 5% CO_2. Then, the membrane was removed, the upper side was washed with PBS, and cells were attached to the lower surface of the filter were fixed, stained with May-Grünwald-Giemsa, mounted on a microscope slide with Cytoseal (Stephens Scientific, Springfield, NJ), and counted. In each experiment, 10 fields/triplicate filter were measured at ×40 magnification. Checkerboard analyses were performed to discriminate between chemotaxis and nondirected migration (chemokinesis) of skin fibroblast cells. In these experiments, cells were placed in the upper chemotactic chambers, and various concentrations of stimuli or buffer were added to the upper or lower wells or to both. Spontaneous migration (chemokinesis) was determined in the absence of chemoattractant or when stimuli were added to either the lower or upper chambers. The cell migratory response to chemotactic stimuli was largely due to chemotaxis and not to chemokinesis. Indeed, a checkerboard analysis, in which chemoattractants above and below the filters varied, resulted in significant migration only when there was a gradient of the factor below the filters.

Proliferation assay

Human skin fibroblasts were serum-starved overnight using DMEM 0.1% BSA, plated at 5×10^3 cells/well in 96-well plates, and incubated with cell culture medium alone or with specific agonists (ATF-uPA [10^{-8} M], $uPAR_{84–95}$ [10^{-9} M], and WKYMVm peptide [10^{-9} M]) or with 10% FBS for 1, 24, 48, 72 h, and 7 d at 37°C, 5% CO_2. At the end of the incubation, 20 μl/well CellTiter-96 was added. After incubation at 37°C for 2 h, the absorbance was determined by an ELISA reader (Bio-Rad) at a wavelength of 490 nm.

In vitro wound healing assay

Sixty-millimeter cell culture dishes were coated with fibronectin (10 μg/ml) or 50 μg/ml poly-L-lysine, as a negative control, for 2 h at 37°C. Coated dishes were blocked with 3 ml of 2 mg/ml BSA for 1 h at 37°C. Normal and SSc fibroblast cells were plated using DMEM containing 2.5% FBS and incubated for 6 h at 37°C to create a confluent monolayer. Cell monolayers were scraped with a p200 pipette tip in a straight line to create a "scratch." The debris was removed, and the edge of the scratch was smoothed by washing cells once with 1 ml growth medium. Normal and SSc fibroblasts were then incubated at 37°C with or without specific agonists (ATF-uPA [10^{-8} M], $uPAR_{84–95}$ [10^{-9} M], and WKYMVm peptide [10^{-9} M]) for 8 and 24 h. Images of the scratched areas were taken at different times, in the same field, as marked by reference points close to the scratch. The healing of the scratch, for each condition, was expressed as a percentage of the original wound measured in three different points.

In situ ELISA

A quantitative analysis of ECM components (fibronectin, collagen type I, and vitronectin) produced by human fibroblasts was performed by an in situ ELISA. Human fibroblasts were plated in a 6-multiwell plate at a density of 5000 cells/well and analyzed after 72 h of culture. Proteins were fixed by acetone/methanol (v/v), for 10 min at 22°C, incubated in 0.5% PBS/BSA and 0.2% Tween 20 for 30 min at 22°C to minimize aspecific binding sites, and washed in PBS. Mouse anti-collagen type I (2 μg/ml), anti-fibronectin (2 μg/ml), and anti-vitronectin (2 μg/ml) were added for 1 h at 22°C. After three washes in PBS, plates were incubated (30 min at 22°C) with HRP anti-mouse IgG. After additional washes in PBS, the substrate was added (1 mg/ml OFD, 0.1 mol/l citrate buffer [pH 5], and 0.006% H_2O_2), and

plates were incubated for 30 min at 37°C in the dark. The reaction was then stopped by 1 N H_2SO_4, and the absorbance was read at 450 nm by a spectrophotometer. Plates without cells and plates coated with purified ECM components at different concentrations were used as controls.

Coimmunoprecipitation

BJ fibroblasts (5×10^6 cells/sample) were plated in 100-mm dishes for 24 h. Cells were lysed in radioimmunoprecipitation assay buffer supplemented with a mixture of proteases and phosphatases inhibitors and incubated with mouse nonimmune serum (Jackson ImmunoResearch Laboratories, Suffolk, UK) and 10% protein A-conjugated Sepharose (GE Healthcare, Milan, Italy) for 2 h at 4°C. After centrifugation, the supernatants were incubated with 2 mg/ml of the R4 monoclonal anti-uPAR Ab, provided by Dr. G. Hoyer-Hansen (Finsen Laboratory, Copenhagen, Denmark), or with nonimmune mouse Igs for 2 h at 4°C and then with 10% protein A–Sepharose for 30 min at room temperature. The immunoprecipitates were washed in radioimmunoprecipitation assay buffer, subjected to 10% SDS-PAGE, and analyzed by Western blot analysis using a polyclonal Ab directed against FPR1.

Determination of ROS

Intracellular ROS generation by adherent cells in a 6-well plate, after loading cells with DCHF-DA, was measured by flow cytometry (FACSCalibur) as described previously (36). The esterified form of DCHF-DA can permeate cell membranes before being deacetylated by intracellular esterases. The resulting compound, dichlorodihydrofluorescein, reacts with ROS, producing an oxidized fluorescent compound, dichlorofluorescein, which can be detected by flow cytometry at a wavelength of 520 nm (FL1). Cell monolayers were treated with medium alone, ATF-uPA (10^{-8} M), $uPAR_{84–95}$ (10^{-9} M), WKYMVm peptide (10^{-9} M), or H_2O_2 (1 mM), as a positive control, for 30 min at 37°C in a humidified 5% CO_2 incubator. Cells were then washed twice, and 5 mM DCHF-DA was added for 30 min in the dark at 37°C. After incubation, cells were washed, trypsinized for immediate analysis, and resuspended in PBS. A total of 10^4 events were acquired for each sample in all cytofluorimetric analysis, and intracellular ROS formation was detected as a result of the oxidation of DCHF. Results are expressed as percentage of increase of mean fluorescence intensity in respect to untreated cells.

Histology and immunohistochemistry

After clinical evaluation, a 3-mm skin punch was taken from the most representative area of each patient affected by SSc and from 10 normal subjects as a control. Each specimen was fixed in 10% buffered formalin, embedded in paraffin, and serial sectioned (4-μm-thick sections). One section for each case was stained with H&E and the others stained by immunohistochemistry (labeled streptavidin biotin standard technique) with anti-FPR1 Ab (1 μg/ml), anti-FPR2 Ab (10 μg/ml), and anti-FPR3 Ab (8 μg/ml). Cells showing a definite black staining confined to the nucleus or cytoplasm were judged positive for FPRs 1, 2, and 3. All slides were examined in a double-blinded fashion by two investigators (M. Mascolo and S. Staibano), and the final staining for each case was expressed as the percentage of positive cells among the total number of counted cells (at least five high-power representative fields).

Statistical analysis

All the experiments were performed at least in triplicate. The results are expressed as mean ± SEM. Values from groups were compared using a paired Student *t* test (37). Differences were considered significant when $p < 0.05$.

Results

Expression of FPR1, FPR2, and FPR3 in human fibroblast cells

We checked the specificity of each primer set on RNAs of KG-1 (human myeloid cell line), K-562 (human myelogenous leukemia cell line), and U-937 (human leukemic monocyte lymphoma cell line) cells. Fig. 1A shows that KG-1 expressed mRNA only for FPR1 (38) and K-562 expressed mRNA only for FPR3, whereas U-937 expressed mRNA both for FPR2 and FPR3 (13).

We examined FPRs expression in skin fibroblasts from 10 normal subjects and 10 SSc patients. The analysis of total RNA by RT-PCR showed expression of all three FPRs (Fig. 1B). The three receptors resulted upregulated in SSc fibroblasts as compared with normal fibroblasts, with a significant increase for FPR2 and FPR3 (fold increase SSc versus normal fibroblasts: FPR1 2.6; FPR2 5.17; and FPR3 6.08) (Fig. 1B).

We then investigated FPR expression in normal and SSc fibroblasts at a protein level. Western blot analysis with specific Abs demonstrated that fibroblasts synthesize all the three FPRs (Fig. 1C). Unexpectedly, we observed a different pattern of increase of FPR protein expression as compared with mRNA levels. Indeed, FPR1 and FPR3 expression increased in SSc fibroblasts as compared with normal fibroblasts (fold increase SSc versus normal fibroblasts: FPR1 4.07; FPR3 1.3; $p < 0.05$), whereas FPR2 was not significantly upregulated (fold increase SSc versus normal fibroblasts 1.02) (Fig. 1C).

These experiments demonstrate that both normal and SSc fibroblasts express FPRs; moreover, SSc fibroblasts show an overexpression as compared with normal cells. It is conceivable that posttranscriptional mechanisms may regulate the expression of these receptors in normal and SSc fibroblasts, causing a different expression pattern at mRNA and protein level.

In vivo expression of FPRs

At histology (H&E staining, in Fig. 2 a representative case), all the enrolled SSc cases (six limited cutaneous and four diffuse cutaneous) showed dermal fibrosis that characteristically involved the subcutis, associated with chronic inflammatory infiltrate, mainly localized at the interface between the deep dermis and subcutis and around vessels (Fig. 2A–C), as compared with normal skin (Fig. 2D). All the evaluated cases showed an increased positivity for FPR1 (Fig. 2E–G), FPR2 (Fig. 2I–K), and FPR3 (Fig. 2M–O), compared with that observed in normal skin (Fig. 2H, 2L, 2P), used as a normal control. FPR1 was found diffusely positive in fibroblasts, endothelial cells, and lymphocytes. FPR2 was expressed in several but not all fibroblasts, whereas FPR3 was seen extensively expressed only in fibroblasts. These data are in agreement with the in vitro observations, showing a lower expression of FPR2, at a protein level, in SSc fibroblasts, compared with FPR1 and FPR3.

Effects of ATF-uPA, $uPAR_{84–95}$, and WKYMVm on human skin fibroblast chemotaxis and adhesion

Chemotaxis contributes to fibrosis by allowing recruitment of fibroblasts, macrophages, and PBMCs to sites of tissue injury (8). FPRs are chemotaxis receptors (11); therefore, we first tested the capability of different FPRs agonists to induce directional migration of normal and sclerotic fibroblasts to investigate a possible role of these receptors in some phases of the disease.

To this aim, we tested the capability of the uPAR-derived chemotactic peptide $uPAR_{84–95}$ and of the synthetic peptide WKYMVm, which are FPRs agonists, to induce directional migration of normal and SSc fibroblasts. We also evaluated the effect of the ATF of uPA (ATF-uPA), able to bind uPAR but devoid of enzymatic activity, which promotes FPRs/uPAR cross-talk (23, 24).

Fig. 3A shows that normal fibroblasts efficiently migrated toward ATF-uPA, $uPAR_{84–95}$, and WKYMVm peptide ($p < 0.001$). SSc fibroblasts showed a less vigorous migratory phenotype and a lower response, as compared with normal fibroblasts, responding significantly only to ATF-uPA and to the WKYMVm peptide ($p < 0.05$).

FPRs also regulate cell adhesion; indeed, their stimulation can enhance mesenchymal stem cell adhesion to ECM protein–coated surfaces (39), whereas their constitutive activation is involved in cell de-adhesion (40). Thus, we tested the effects of FPRs agonists on normal and SSc fibroblast adhesion to type I collagen. Stimulation with ATF-uPA, $uPAR_{84–95}$, and WKYMVm peptide induced a significant detachment from collagen in normal fibroblasts, whereas it did not exert any effect on SSc fibroblasts (Fig. 3B).

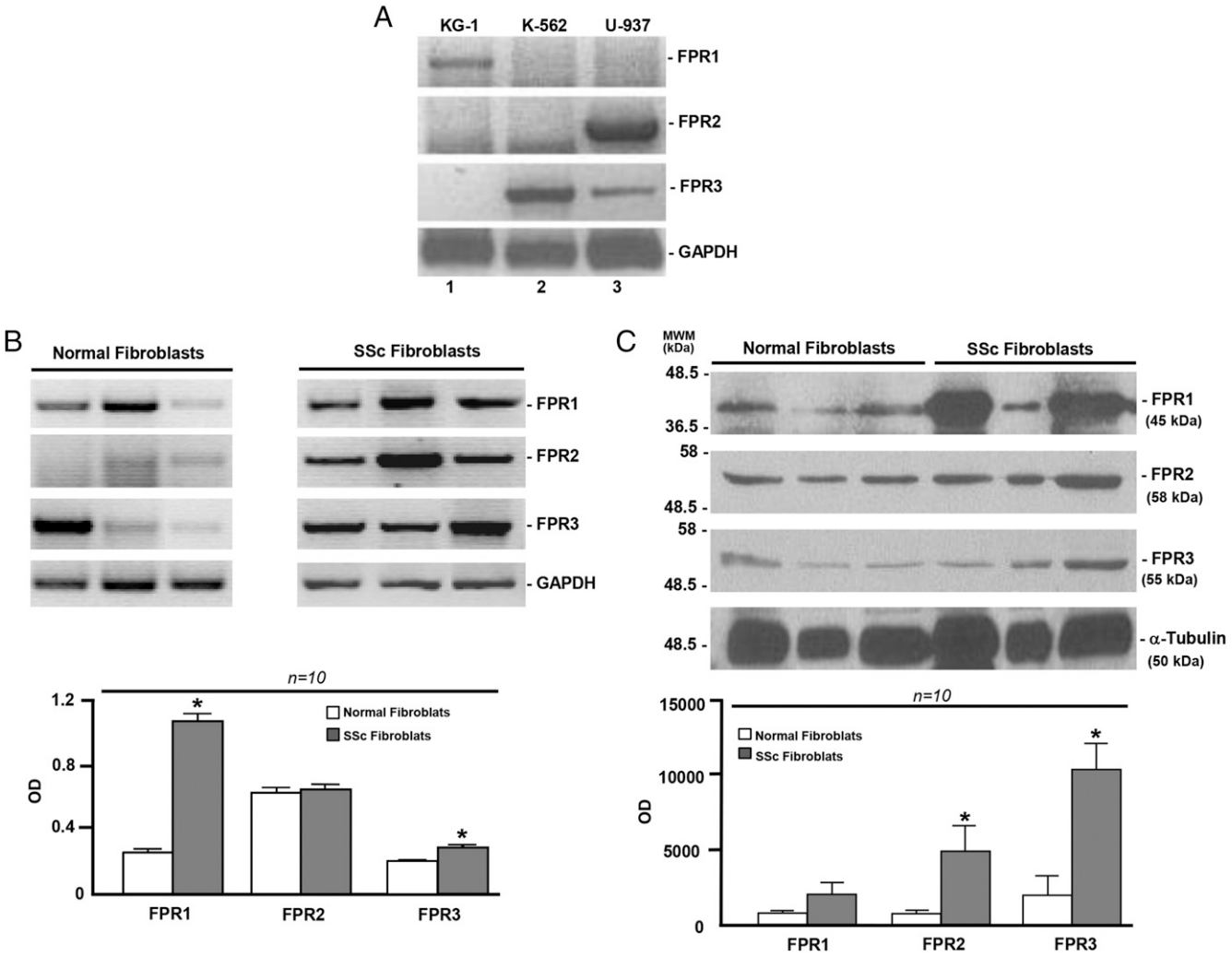

FIGURE 1. (**A**) mRNA expression of FPRs in human leukemia cell lines. Total RNA was isolated and retrotrascribed from KG-1 cell line as a positive control for FPR1 (*lane 1*), K-562 cell line as a positive control for FPR3 (*lane 2*), and U-937 cell line as a positive control for FPR2 and FPR3 (*lane 3*). cDNAs were amplified by 40 PCR cycles in the presence of FPR1-, FPR2-, and FPR3-specific primers and GAPDH primers as loading control. (**B**) mRNA expression of FPRs in normal and SSc fibroblasts. Total RNA was isolated from skin fibroblasts derived from 10 normal subjects and 10 SSc patients; RNA was retrotranscribed, and cDNAs were amplified by 40 PCR cycles in the presence of FPR1-, FPR2-, and FPR3-specific primers and GAPDH primers as loading control. (B) is representative of the results obtained in three normal and three SSc subjects. Normalization using densitometric analysis of the FPR expression in normal (white columns) and SSc (gray columns) fibroblasts show that SSc fibroblasts overexpress FPR2 and FPR3 as compared with normal fibroblasts. Values are mean ± SEM of 10 normal and 10 SSc subjects. (**C**) Western blot analysis of FPRs in normal and SSc fibroblasts. Skin fibroblasts derived from 10 normal subjects and 10 SSc patients were lysed in Triton X-100, and 50 μg total protein was analyzed by Western blot with anti–FPR1-, anti–FPR2-, and anti–FPR3-specific Abs and then with α-tubulin Abs for loading control. Normalization with α-tubulin using densitometric analysis of the FPR protein levels show a significant increase of FPR1 and FPR3 in SSc fibroblasts (gray columns) as compared with normal fibroblasts (white columns). Values are mean ± SEM of 10 normal and 10 SSc subjects. $*p < 0.05$.

These results suggest that migration mediated by FPRs is impaired in SSc fibroblasts, in particular in response to the chemotactic $uPAR_{88–95}$ peptide. Moreover, SSc fibroblasts are less adhesive than normal fibroblasts to type I collagen, although not significantly, and do not respond to FPRs agonists.

Effects of ATF-uPA, $uPAR_{84–95}$, WKYMVm on human skin fibroblast proliferation

It has been previously described that fibroblasts from idiopathic pulmonary fibrosis display a less vigorous proliferation activity (36). Thus, we analyzed the growth properties of normal and SSc fibroblasts in the presence of 10% FBS. Interestingly, proliferation of SSc fibroblasts was significantly lower as compared with normal cells at each point of the proliferation curve (Fig. 3C).

Because overexpression of FPR1 could confer a more invasive and proliferative phenotype (41), the effect of different uPAR and FPRs agonists on cell proliferation was investigated. Cells were incubated with ATF-uPA, $uPAR_{84–95}$, and WKYMVm peptide and cell number was measured at 72 h (Fig. 3D). Proliferation of normal fibroblasts significantly increased in response to all specific ligands; by contrast, only ATF-uPA was able to act in a significant manner in SSc fibroblasts (Fig. 3D).

These results indicate that SSc fibroblasts proliferate less than normal cells and, despite the overexpression of FPRs, poorly respond to their ligands, except for ATF-uPA, that, indeed, only indirectly can stimulate FPRs.

Effects of ATF-uPA, $uPAR_{84–95}$, and WKYMVm on normal and SSc skin fibroblast wound healing

During normal healing of skin, connective tissue is repaired exclusively through the action of fibroblasts, which migrate into the wound site (42). In in vitro wound healing assays, both normal and

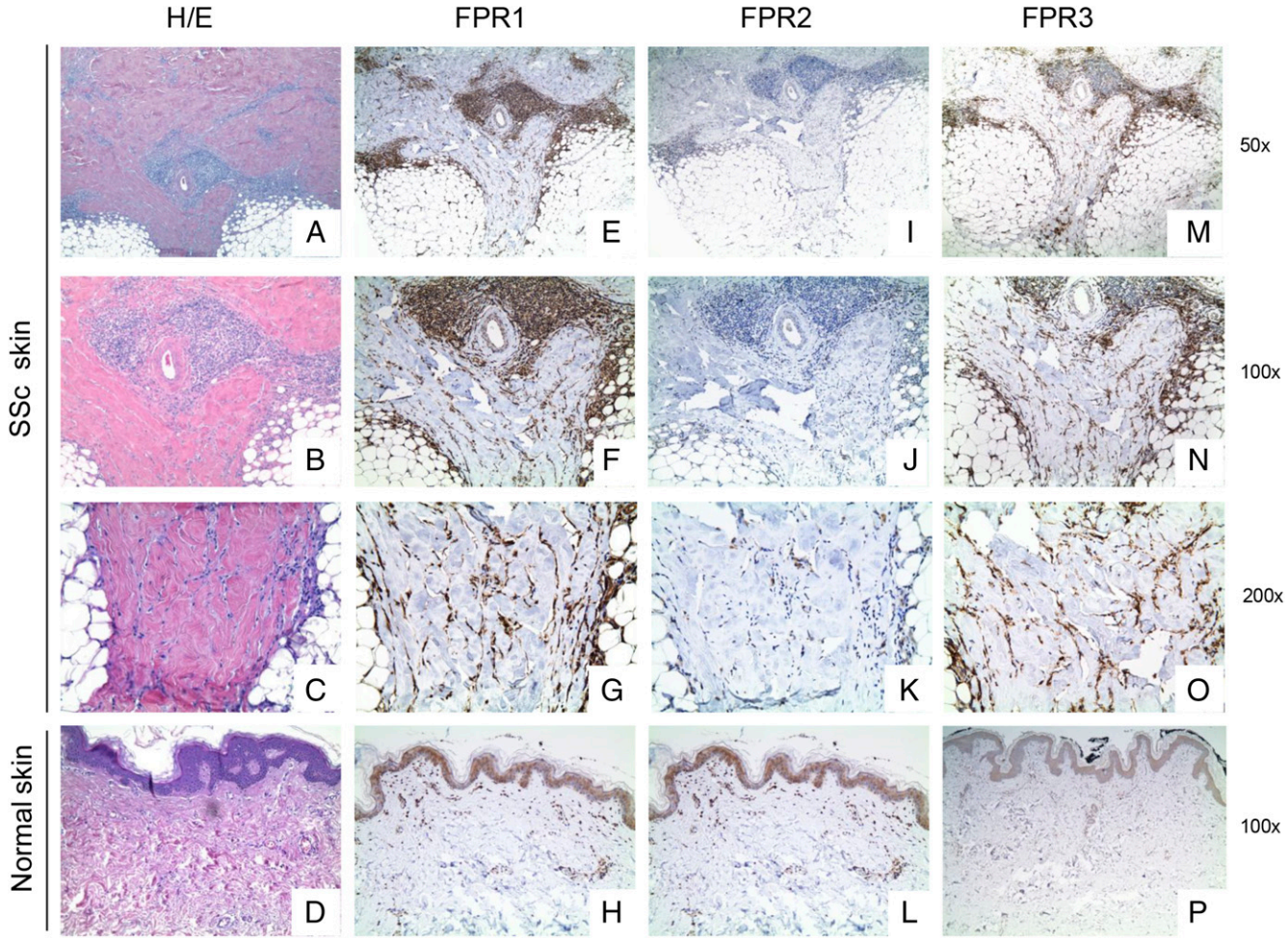

FIGURE 2. Histological expression of FPRs in skin biopsies. (**A**–**C**) Histologic appearance of a localized scleroderma. [H&E; original magnification ×50 (A), ×100 (B), and ×200 (C)]. (**D**) Histologic appearance of normal skin (H&E; original magnification ×100). (**E**–**G**) Immunostaining for FPR1 in a localized scleroderma. Overexpression of FPR1 was observed in fibroblasts, endothelial cells, and lymphocytes [original magnification ×50 (E), ×100 (F), and ×200 (G)]. (**H**) Immunostaining for FPR1 in normal skin. Weak expression of FPR1 was observed in fibroblasts, lymphocytes, and endothelial cells (original magnification ×100). (**I**–**K**) Immunostaining for FPR2 in a localized scleroderma. Only a minority of fibroblasts resulted positive for FPR2 [original magnification ×50 (I), ×100 (J), ×200 (K)]. (**L**) Immunostaining for FPR2 in normal breast skin in normal skin. Only two fibroblasts resulted positive for FPR2 (original magnification, ×100). (**M**–**O**) Immunostaining for FPR3 in a localized scleroderma. Most fibroblasts show positivity for FPR3. Lymphocytes and endothelial cells were negative [original magnification ×50 (M), ×100 (N), ×200 (O)]. (**P**) Immunostaining for FPR3. Some fibroblasts showed positivity for FPR3. Lymphocytes and endothelial cells were negative (original magnification ×100).

SSc fibroblasts were able to close in a significant manner the scratch at 8 and 24 h, compared with time 0, considered as 100% (Fig. 4A). However, the efficiency in wound healing by SSc cells was higher at 24 h, compared with normal cells ($p < 0.05$).

We then evaluated the effects of ATF-uPA, $uPAR_{84–95}$, and WKYMVm peptide in wound healing assays on normal and SSc fibroblasts. The size of the gaps in the presence of the different FPRs agonists was measured at different time points (0, 8, and 24 h) and compared with the gap size in the absence of agonists, considered as 100%. Both in normal and SSc fibroblast, wound healing efficiency was increased by all the stimuli at 24 h. At 8 h, ATF-uPA, $uPAR_{84–95}$, and WKYMVm peptide improved normal fibroblasts wound healing, whereas only the WKYMVm peptide exerted a significant effect on SSc fibroblasts ($p < 0.05$) (Fig. 4B).

Thus, SSc fibroblasts show an increased basal motogenic activity as compared with normal fibroblasts, as demonstrated previously (43); however, except for the WKYMVm peptide, SSc fibroblast response to FPRs agonists is strongly delayed.

Effects of ATF-uPA, $uPAR_{84-95}$ and WKYMVm on normal and SSc skin fibroblast ECM deposition

SSc is characterized by the overproduction of ECM proteins (44). To investigate the possibility that deposition of ECM could be regulated by FPR stimulation, we evaluated fibronectin, collagen type I, and vitronectin secretion by in situ ELISAs in basal condition and upon challenge with ATF-uPA, $uPAR_{84–95}$, and WKYMVm, in normal and SSc skin fibroblasts.

SSc fibroblasts showed only a slight increase in fibronectin production in respect to normal fibroblasts; by contrast, collagen type I and vitronectin deposition was significantly increased in SSc fibroblasts ($p < 0.05$). Both cell types significantly increased matrix deposition in response to FPRs stimulation (Fig. 4C).

Expression of myofibroblast associated markers on human skin fibroblasts and their induction by FPR stimulation

In rheumatoid arthritis, fibroblast activation is characterized also by the induction of the uPA pathway (45), even though we could observe uPA increase only in localized SSc forms (29). uPA is able to cleave uPAR (20, 22, 23). uPA-mediated uPAR cleavage

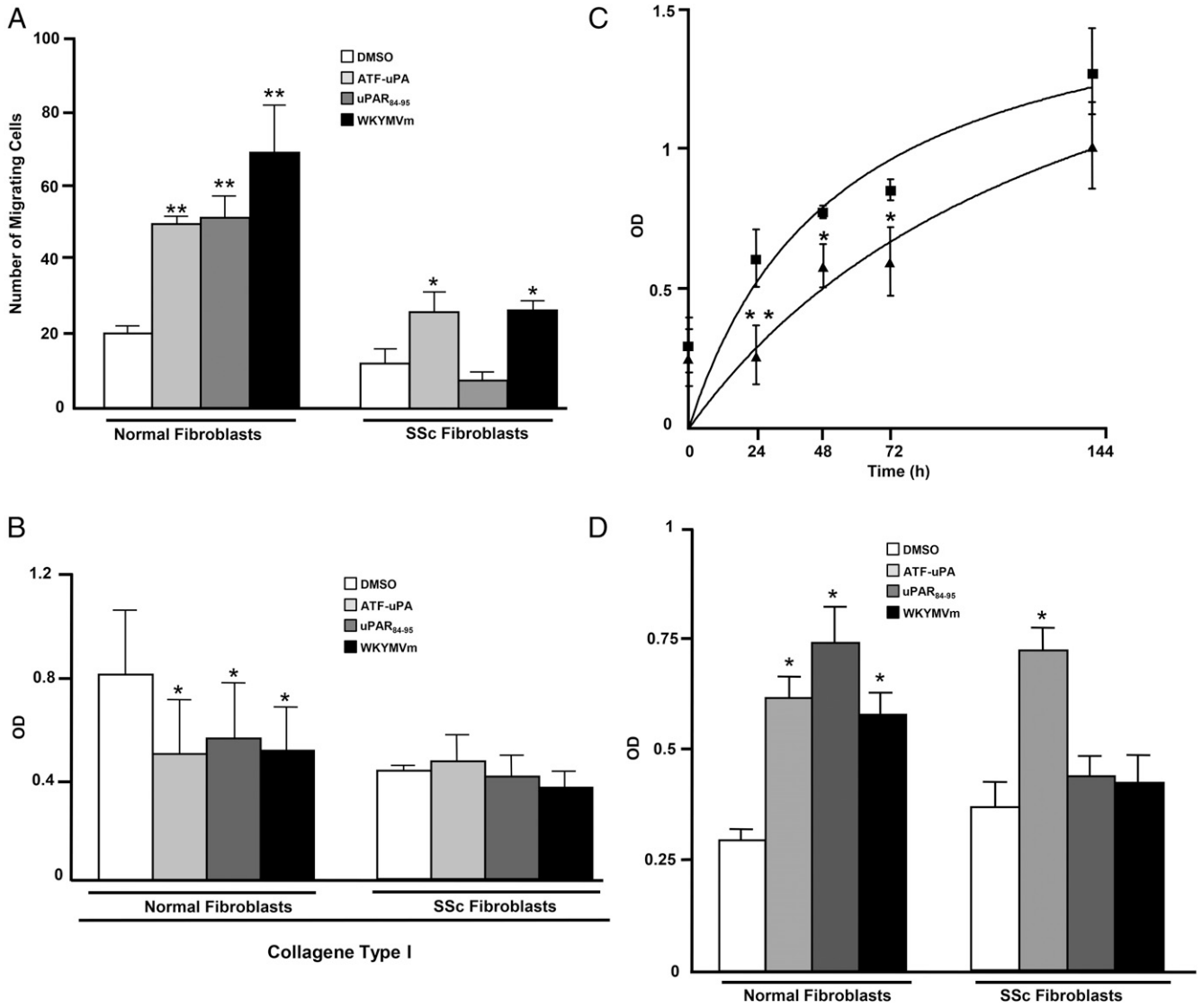

FIGURE 3. (**A**) Effects of ATF-uPA, $uPAR_{84–95}$, and WKYMVm on normal and SSc skin fibroblast chemotaxis. Skin fibroblasts from normal subjects and SSc patients were allowed to migrate in response to cell medium alone (white column) or ATF-uPA (10^{-9} M) (light gray column), $uPAR_{84–95}$ peptide (10^{-9} M) (dark gray column), or WKYMVm peptide (10^{-8} M) (black column) for 6 h at 37°C in a humidified (5% CO_2) incubator. (**B**) Effects of ATF-uPA, $uPAR_{84–95}$, and WKYMVm on normal and SSc skin fibroblast adhesion. Skin fibroblasts from normal subjects and SSc patients were plated onto type I collagen–coated wells and allowed to adhere in response to cell medium alone (white column) or ATF-uPA (10^{-9} M) (light gray column), $uPAR_{84–95}$ peptide (10^{-9} M) (dark gray column), or WKYMVm peptide (10^{-8} M) (black column) for 1 h at 37°C in a humidified (5% CO_2) incubator. Attached cells were fixed and stained with crystal violet; the stain was eluted and the absorbance (OD) was determined by an ELISA reader at a wavelength of 540 nm. (**C**) Proliferation of normal and SSc skin fibroblast. Normal and SSc skin fibroblasts were grown in 96-well plates for 1, 24, 48, 72, and 144 h in the presence of 10% FCS at 37°C in a humidified (5% CO_2) incubator. At the end of the incubation, 20 μl/well Cell Titer 96 reagent was added, and absorbance (OD) was determined by ELISA reader at a wavelength of 490 nm. (**D**) Effects of ATF-uPA, $uPAR_{84–95}$, and WKYMVm on normal and SSc skin fibroblast proliferation. Normal and SSc skin fibroblasts were grown in 96-well plates for 72 h at 37°C in a humidified (5% CO_2) incubator in the presence of medium alone (white column), ATF-uPA(10^{-9} M) (light gray column), $uPAR_{84–95}$ (10^{-9} M) (dark gray column), and WKYMVm peptide (10^{-8} M) (black column) at 37°C in a humidified (5% CO_2) incubator. At the end of the incubation, 20 μl/well Cell Titer 96 reagent was added, and absorbance (OD) was determined by ELISA reader at a wavelength of 490 nm. Values are mean ± SEM of six experiments. *$p < 0.05$, **$p < 0.001$.

results in the expression on the cell membrane of a truncated form of the receptor, which can contain (DII-DIII-$uPAR_{88–92}$) or not (DII-DIII-uPAR) the chemotactic peptide (residues 88–92) able to interact with FPRs and to regulate their signal (26). uPAR cleavage contributes to the impaired angiogenesis observed in SSc patients (30).

Thus, we investigated DII-DIII-$uPAR_{88–92}$ expression in normal and SSc fibroblasts by Western blot analysis, using a specific Ab directed against the Ser^{88}-Arg-Ser-Arg-Tyr^{92} sequence (46). Fig. 5A shows that SSc fibroblasts markedly overexpressed DII-DIII-$uPAR_{88–92}$ (fold increase SSc fibroblasts versus normal cells: 4.7; $p < 0.05$).

Many cultured cell types, including fibroblasts and endothelial cells, do not synthesize in basal conditions, vitronectin, which characterizes the myofibroblast phenotype (19), and directly binds uPAR, inducing a specific cell signaling (18). We have therefore investigated the expression of vitronectin in normal and SSc fibroblasts by Western blot analysis. SSc fibroblasts significantly overexpressed vitronectin, as compared with normal cells (fold increase SSc fibroblasts versus normal cells: 4.26; $p < 0.05$), supporting the hypothesis of a transition of SSc fibroblasts toward the myofibroblast phenotype (Fig. 5B).

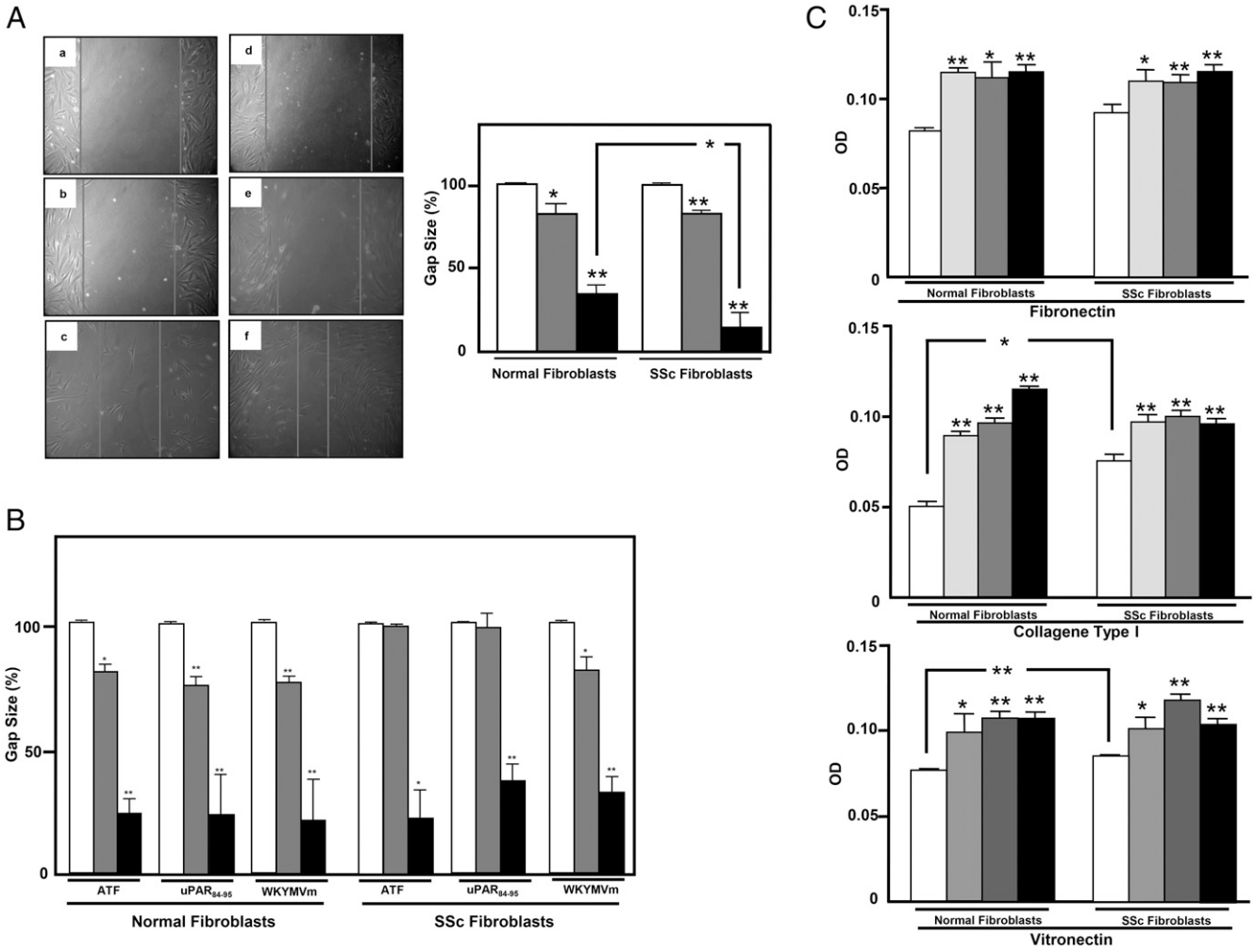

FIGURE 4. (**A**) In vitro wound healing assay of normal and SSc fibroblasts. Migration was measured using a wound healing assay. Fibroblasts were cultured on fibronectin until confluence, and a linear scrape was made across the cell layer. Migration of normal (A**a**–A**c**) and SSc (A**d**–A**f**) fibroblasts was monitored at time 0 [(Aa and Ad) white columns], 8 h [(Ab and Ae) light gray columns], and 24 h [(Ac and Af) black columns]. Original magnification ×10. Three independent measurements of the scratch were performed; scratch size is expressed as a percentage of the original wound size at time 0, considered as 100%. Values are mean ± SEM of three experiments. (**B**) Effects of ATF-uPA, $uPAR_{84–95}$, and WKYMVm on normal and SSc skin fibroblast on wound healing. Skin fibroblasts from normal subjects and SSc patients were allowed to migrate in response to cell medium alone, ATF-uPA (10^{-9} M), $uPAR_{84–95}$ peptide (10^{-9} M), or WKYMVm peptide (10^{-8} M), for 0 h (white columns), 8 h (light gray columns), and 24 h (dark gray columns) at 37°C in a humidified (5% CO_2) incubator. Scratch size is expressed as a percentage of the control wound obtained in the absence of agonist at the same time point (100%). Values are mean ± SEM of three experiments. (**C**) Effects of ATF-uPA, $uPAR_{84–95}$, and WKYMVm on normal and SSc skin fibroblast ECM deposition. Normal and SSc skin fibroblasts were grown in 6-multiwell plates in the presence of medium alone (white column), ATF-uPA (10^{-9} M) (light gray column), $uPAR_{84–95}$ (10^{-9} M) (dark gray column), and WKYMVm peptide (10^{-8} M) (black column) at 37°C in a humidified (5% CO_2) incubator for 72 h at 37°C in a humidified (5% CO_2) incubator. Proteins were fixed by acetone/methanol and incubated with anti-fibronectin, anti-collagen type I, and anti-vitronectin Abs for 1 h at 22°C. Absorbance (OD) was determined by ELISA reader at a wavelength of 490 nm. Values are mean ± SEM of six experiments. $*p < 0.05$, $**p < 0.001$.

Then, we investigated the expression of α-SMA, a typical marker of myofibroblast phenotype (8). Western blot analysis, using a specific Ab against α-SMA, showed an increased expression in cell lysates from SSc fibroblasts as compared with control (fold increase SSc fibroblasts *vs* normal cells: 2.97; $p < 0.05$) (Fig. 5C).

To investigate whether this SSc cell phenotype was linked to the activation of FPRs, we measured the expression of α-SMA in control fibroblasts upon challenge with ATF-uPA, $uPAR_{84–95}$, and WKYMVm peptide. As shown in Fig. 5D, α-SMA expression was strongly induced by specific ligands at 18 h in normal fibroblasts ($p < 0.05$). No increase, except for ATF-uPA, was observed when SSc fibroblasts were stimulated in the same conditions.

In SSc fibroblasts, the expression of $\alpha_v\beta_5$ and $\alpha_v\beta_3$ integrins is upregulated and correlates with the transition of fibroblasts into myofibroblasts (47, 48). uPAR, through its Ser^{88}-Arg-Ser-Arg-Tyr^{92} sequence, mediates FPR cross-talk with $\alpha_v\beta_5$ integrin, thus inducing cell migration and cytoskeletal rearrangements (49). Therefore, we also investigated $\alpha_v\beta_5$ expression and regulation by FPR agonists in normal and SSc fibroblasts. Fig. 5D shows that $\alpha_v\beta_5$ expression was strongly induced at 18 h in normal fibroblasts by ATF-uPA and WKYMVm peptide ($p < 0.05$). When SSc fibroblasts were stimulated in the same conditions, an increase was observed with ATF-uPA ($p < 0.05$), and only WKYMVm peptide exerted a stronger effect ($p < 0.05$).

Effects of ATF-uPA, $uPAR_{84–95}$, and WKYMVm peptides on human skin fibroblast ROS production

There are accumulating evidences suggesting a role of the oxidative stress in the pathogenesis of SSc (50); indeed, it has been shown

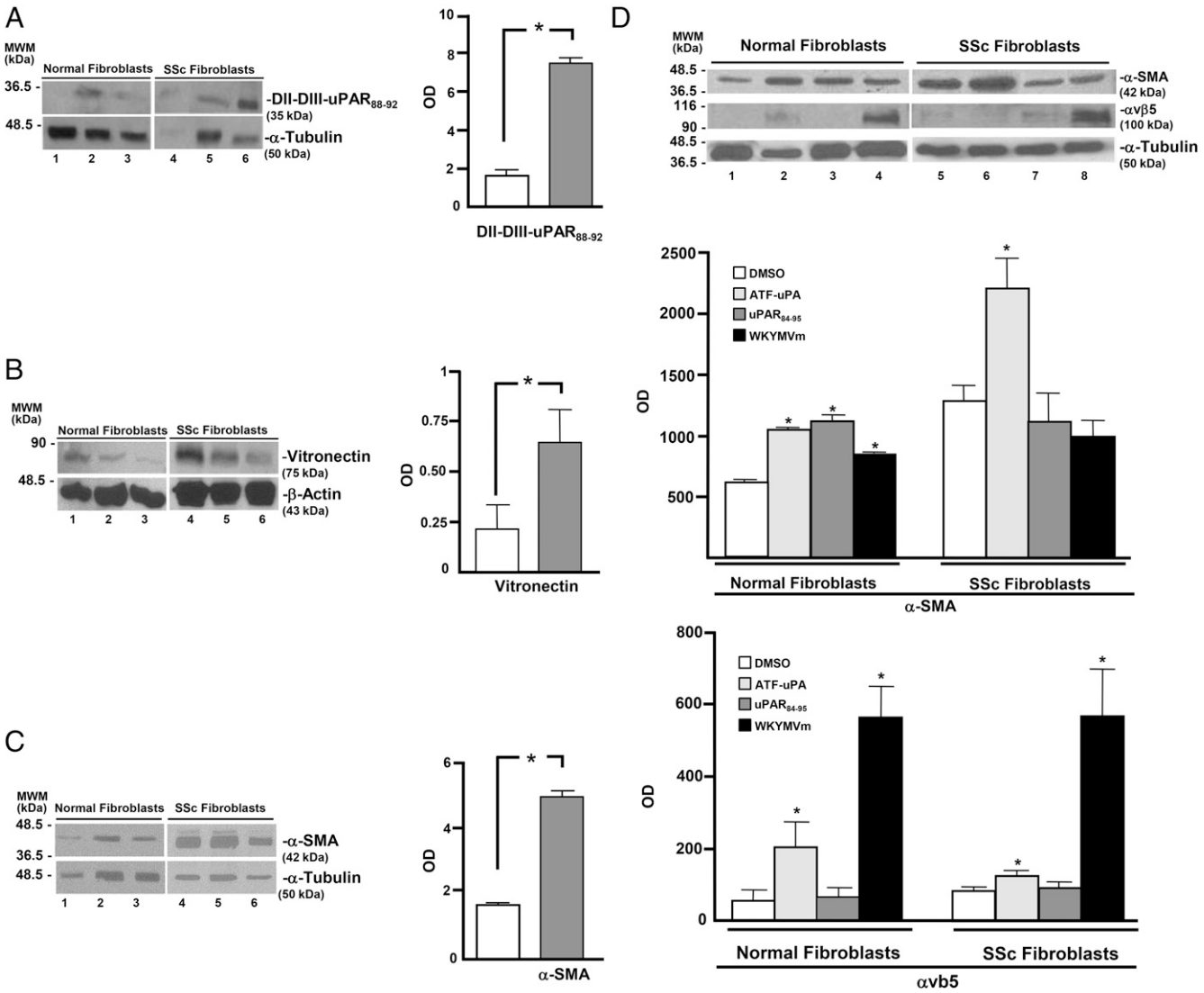

FIGURE 5. (**A**) Western blot analysis of DII-DIII-uPAR$_{88–92}$ expression in normal and SSc skin fibroblasts. Normal (*lanes 1–3*) and SSc (*lanes 4–6*) skin fibroblasts were lysed in Triton X-100, and 50 μg total protein was analyzed by Western blot with an anti–uPAR$_{84–95}$-specific Ab; three representative cases are shown. Densitometric analysis and normalization to α-tubulin of the DII-DIII-uPAR$_{88–92}$ expression in normal (white column) and SSc fibroblasts (gray column) are also shown. (**B**) Western blot analysis of vitronectin expression in normal and SSc skin fibroblasts. Normal (*lanes 1–3*) and SSc (*lanes 4–6*) skin fibroblasts were lysed in Triton X-100, and 50 μg total protein was analyzed by Western blot with an anti–vitronectin-specific Ab; three representative cases are shown. Densitometric analysis and normalization to α-tubulin of vitronectin expression in normal (white column) and SSc fibroblasts (gray column) are also shown. (**C**) Western blot analysis of α-SMA and expression in normal and SSc skin fibroblasts. Normal (*lanes 1–3*) and SSc (*lanes 4–6*) skin fibroblasts were lysed in Triton X-100, and 50 μg total protein was analyzed by Western blot with an anti–α-SMA-specific Ab. Three representative cases are shown. Densitometric analysis and normalization to α-tubulin of the α-SMA expression in normal (white column) and SSc fibroblasts (gray column) are also shown. (**D**) Effects of ATF-uPA, uPAR$_{84–95}$, and WKYMVm in normal and SSc skin fibroblasts expression of α-SMA and $\alpha_v\beta_5$ integrin. Normal (*lanes 1–4*) and SSc (*lanes 5–8*) skin fibroblasts were treated with medium alone (*lanes 1* and *5*) or with ATF-uPA (10^{-9} M) (*lanes 2* and *6*), uPAR$_{84-95}$ (10^{-9} M) (*lanes 3* and *7*), or WKYMVm peptide (10^{-8} M) (*lanes 4* and *8*) for 18 h at 37°C in a humidified (5% CO_2) incubator. At the end of the incubation, cells were lysed in Triton X-100, and 50 μg total protein was analyzed by Western blot with an anti–α-SMA and $\alpha_v\beta_5$ integrin–specific Ab; a representative case of one normal and one SSc patient is shown. Densitometric analysis and normalization to α-tubulin of the α-SMA and $\alpha_v\beta_5$ integrin expression in normal and SSc fibroblasts after treatment with medium alone (white column), ATF-uPA (10^{-9} M) (light gray column), uPAR$_{84–95}$ (10^{-9} M) (dark gray column), or WKYMVm peptide (10^{-8} M) (black column) are also shown. Values are mean ± SEM of 10 normal and 10 SSc subjects. *$p < 0.05$.

that ROS contribute to the persistent fibrotic phenotype of SSc fibroblasts (43) and that antioxidants, such as epigallocatechin-3-gallate, can reduce ECM production, function, and activity of dermal fibroblasts from SSc patients (44).

Several studies have described, among the various properties of FPRs, the capability to generate ROS generation upon binding to their specific ligands (50). Interestingly, SSc neutrophils may induce local production of ROS upon fMLF stimulation in endothelium (51).

Thus, we evaluated the effects of FPR activation on ROS release in normal and SSc fibroblasts. Normal and SSc fibroblasts were tested, by flow cytometry analysis, for the ability to induce ROS generation. The basal level of fluorescence was determined in both cell types after loading with DCHF-DA. DCHF-DA–loaded normal and SSc fibroblasts did not show a different level of basal ROS production (Fig. 6A). After cell stimulation with H_2O_2 (1 mM), normal and SSc fibroblasts showed a similar, significant increase in ROS production (Fig. 6B).

To investigate whether FPR stimulation may have a role in ROS production, we evaluated ROS levels after stimulation with specific agonists of uPAR/FPRs. The intracellular ROS levels were determined after 30 min of stimulation with ATF-uPA, $uPAR_{84–95}$, and WKYMVm peptide (Fig. 6C) and compared with unstimulated cells. As shown in Fig. 6C, normal fibroblasts responded in a significant manner to all the three stimuli ($p < 0.05$), whereas in SSc fibroblasts, only the pan-FPR agonist WKYMVm peptide significantly induced ROS generation, thus suggesting that uPAR/FPR cross-talk could be impaired in SSc fibroblasts.

Indeed, both intact (52) and cleaved DII-DIII-$uPAR_{88–92}$, either on the cell membrane (53) or in a soluble form (27), can interact with FPRs in many cell types (20, 23). To investigate whether such interaction could also occur in fibroblast cells, a pull-down experiment was carried out in human skin fibroblasts from the BJ cell line, constitutively expressing all FPRs and both forms of uPAR (data not shown). In BJ cells, immunoprecipitation with a monoclonal anti-uPAR Ab and Western blot analysis of the immunoprecipitate with polyclonal anti-FPR1 Abs revealed a band corresponding to FPR1 that was absent in the same lysate

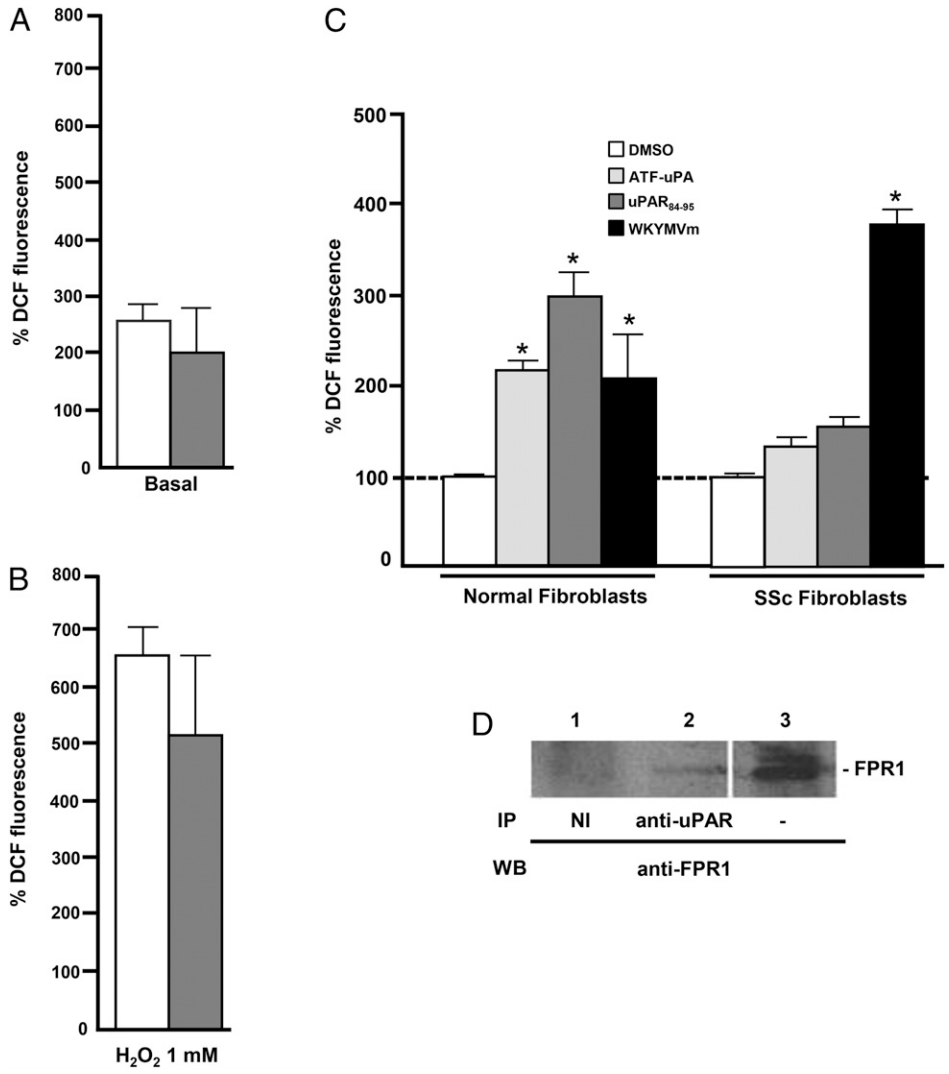

FIGURE 6. (**A**) Intracellular oxidation in normal and SSc fibroblasts in basal conditions. Normal ($n = 10$, white column) and SSc ($n = 10$, gray column) skin fibroblasts were plated in a 6-well plate. Cells were untreated or treated with H_2O_2 (1 mM) for 30 min at 37°C in the dark. At the end of incubation, cells were washed with PBS and loaded with DCHF-DA (5 mM) for 30 min; then, ROS release was measured by flow cytometry at a wavelength of 520 nm (FL1). Results are expressed as percentage of increase of mean fluorescence intensity DCHF-DA–loaded cells, as compared with DCHF-DA–unloaded cells. (**B**) Normal ($n = 10$, white column) and SSc ($n = 10$, gray column) skin fibroblasts were plated in a 6-well plate. Cells were untreated or treated with H_2O_2 (1 mM) for 30 min at 37°C in the dark. At the end of incubation, cells were washed with PBS and loaded with DCHF-DA (5 mM) for 30 min; then, ROS release was measured by flow cytometry at a wavelength of 520 nm (FL1). Results are expressed as percentage of increase of mean fluorescence intensity of H_2O_2-stimulated over H_2O_2-unstimulated cells. (**C**) Effects of ATF-uPA, $uPAR_{84–95}$, and WKYMVm on ROS production in normal and SSc skin fibroblasts. Normal and SSc fibroblasts were treated with medium alone (white column), ATF-uPA (10^{-9} M) (light gray column), $uPAR_{84–95}$ (10^{-9} M) (dark gray column), and WKYMVm peptide (10^{-8} M) (black column) for 30 min at 37°C in a humidified 5% CO_2 incubator. Cells were then washed twice, and 5 mM DCHF-DA was added for 30 min in the dark at 37°C. At the end of the incubation, cells were washed, trypsinized, and resuspended in PBS for flow cytofluorimetric analysis. A total of 10^4 events were acquired for each sample in all cytofluorimetric analysis, and intracellular ROS formation was detected as a result of the oxidation of DCHF. DCHF-DA–loaded H_2O_2-unstimulated cells were considered the 100% of the dichlorofluorescein (DCF) fluorescence. *$p < 0.05$. (**D**) uPAR coimmunoprecipitation with FPR1. BJ cell lysates were immunoprecipitated with the R4 anti-uPAR mAb (*lane 2*) or with nonimmune serum (*lane 1*). The immunoprecipitated samples were electrophoresed on 10% SDS-PAGE and analyzed by Western blot analysis with an anti-FPR1 Ab. Nonimmunoprecipitated cell lysates were subjected to Western blot analysis with the anti-FPR1 Ab (*lane 3*) as a loading control.

immunoprecipitated with nonimmune Igs. As a control, a corresponding band was evidenced in BJ total cell lysates subjected to Western blot analysis with anti-FPR1 Abs (Fig. 6C). Therefore, a structural interaction between uPAR and FPR1 can occur in the fibroblast cell type and exert functional effects.

Discussion

The importance of the FPRs in different inflammatory conditions and their involvement in innate immune responses is well established (54). However, their involvement in SSc pathogenesis has never been investigated. To our knowledge, our data demonstrate for the first time both in vivo and in vitro that human skin fibroblasts express FPRs and that SSc fibroblasts ovreexpress FPR1, FPR2, and FPR3 (Fig. 1B, 1C). FPRs could be involved in the pathogenesis of SSc through different mechanisms, including the interaction with the uPA/uPAR system, as previously demonstrated in epithelial cells (26). Adhesion, proliferation, and chemotaxis assays showed that ligands of uPAR and FPRs, including the $uPAR_{84–95}$ peptide, exerted a significant effect on normal skin fibroblasts (Fig. 3). Despite the overexpression of FPRs, SSc fibroblasts were less responsive to their ligands, except for ATF-uPA, which exerted the same proliferative effect as in normal fibroblasts.

Fibroblasts isolated from clinically affected, but not unaffected, areas of SSc patients are characterized by elevated adhesion to and contraction of ECM (47). Differently from bronchial human fibroblasts (55), we found that dermal fibroblasts from SSc were not more adherent to type I collagen. However, their adhesion was insensitive to FPR activation, responsible for both deadhesion and proadhesion activity in different cell types (39, 40).

These results suggest that FPRs are less functional in SSc fibroblasts in respect to normal fibroblasts. Indeed, FPRs can be inactivated and/or desensitized by several mechanisms, depending on ligand engagement, activation of other chemotaxis receptors, internalization, or phosphorylation (11). In the presence of inactive FPRs, ATF-uPA is less efficient in inducing cell migration in SSc fibroblasts, but it is still able to stimulate cell proliferation to the same extent than normal fibroblasts, probably by activating other signaling partners, such as, for instance, integrins (52). Fibroblasts from lesional areas of SSc possess a motogenic phenotype and increased ability to produce type I collagen (56). Accordingly, we showed that SSc fibroblasts migrated faster in wound healing assays and secreted more ECM proteins than normal cells (Fig. 4). Moreover, incubation with FPRs agonists increased the rate of wound healing and ECM deposition in both normal and SSc fibroblasts.

Interestingly, previous studies have evidenced that retaining full-length uPAR is essential for regulating myofibroblast differentiation and that the cleavage/inactivation of uPAR is a crucial step in the fibroblast-to-myofibroblast transition (57). This hypothesis has been supported by the observation that uPAR deletion induces, in a murine model, pulmonary fibrosis and peripheral microvasculopathy (58). On this basis, we also investigated whether SSc fibroblasts, which show an increased membrane expression of cleaved uPAR, exhibited characteristics suggesting a myofibroblast transition. Indeed, we demonstrated increased vitronectin production from SSc fibroblasts, which is associated to fibrosis and myofibroblast phenotype (25).

Myofibroblasts also show increased α-SMA expression, which represents the key feature of cellular response to injury and of an uncontrolled activated phenotype. Indeed, we observed increased expression of α-SMA in SSc fibroblasts and showed that uPAR/FPRs stimulation and cross-talk was able to induce, in normal fibroblasts, an increased expression of α-SMA. Thus, we could hypothesize that FPRs/uPAR could be involved in the arising of myofibroblast features. However, α-SMA overexpressing SSc fibroblasts failed to still respond to FPR agonists and increased their α-SMA production only in response to ATF-mediated uPAR stimulation. We can suggest that, as in SSc fibroblasts proliferation, FPRs and their cross-talk with uPAR are inactivated, but uPAR is still active, most probably through the engagement of different membrane partners. Indeed, in corneal fibroblasts, uPA treatment is able to induce myofibroblast differentiation by activating $\alpha_v\beta_3$ and $\alpha_v\beta_5$ integrins and promoting their binding to vitronectin, which is overexpressed in corneal fibroblasts (59) as well as in SSc fibroblasts (Fig. 3B).

$\alpha_v\beta_3$ integrin and $\alpha_v\beta_5$ are upregulated in SSc fibroblasts (60, 61) and contribute to the pathogenesis of fibrotic disorders by promoting cell migration, vitronectin endocytosis, and TGF-β autocrine signaling (47). αvβ5 expression can be upregulated by uPAR activation, thus increasing cell adhesion and migration (62). We documented that uPAR engagement by ATF-uPA was able to increase $\alpha_v\beta_5$ expression also in normal and in SSc fibroblasts; in addition, FPR stimulation determined a stronger effect in both cell types (Fig. 4D).

Integrin-mediated signals contribute to the fibrotic phenotype of SSc fibroblasts by the same molecular mechanisms that operate downstream ROS (43). Indeed, several years ago, many groups (10, 43, 44, 63) suggested that the pathogenesis of scleroderma was linked to the generation of a large excess of ROS. The scleroderma phenotype at the cellular level is characterized by oxidative stress associated with the accumulation of large amounts of ROS in fibroblasts. ROS are key cell transducers of fibroblast proliferation and collagen-gene expression. Furthermore, several studies in animal models of scleroderma have confirmed the relevance of oxidative stress in the pathogenesis of the fibrotic processes (57). It has been previously demonstrated that uPA activation is able to induce, in a model of arterial injury, ROS generation (64). Interestingly, Barnes et al. (65) showed that neutrophil stimulation with a specific FPR agonist resulted in increased ROS generation in SSc neutrophils. To this regard, we finally analyzed the effects of uPAR/FPRs stimulation on fibroblasts ROS production, showing that normal fibroblasts significantly respond to all the agonists. On the contrary, only the WKYMVm peptide seems to be a potent stimulus for SSc fibroblasts.

In conclusion, to our knowledge, our data show, for the first time, that FPRs and their cross-talk with the uPA/uPAR system are involved in the activation of normal fibroblasts proliferation, migration, and induction of a myofibroblast phenotype through ROS generation, matrix deposition, and α-SMA overexpression. This supports the hypothesis that the SSc progressive fibrosis could be linked to aberrant activation of FPRs signaling. We indeed suggest that, although in normal fibroblasts a cross-talk between the FPRs and uPAR occurs, as demonstrated by coimmunoprecipitation experiments and by significant response to the $uPAR_{88–95}$ peptide in the adhesion, migration, and proliferation assays, in SSc fibroblasts a condition of inactivation probably contribute to the reduced response observed in vitro (Fig. 3). This desensitization/inactivation could be due to the increased membrane expression of $uPAR_{88–92}$ observed in vitro in SSc fibroblasts. Moreover, in SSc fibroblasts, uPAR signaling is still active in inducing α-SMA production, whereas FPRs are engaged preferentially in ROS generation.

SSc is a heterogeneous disease in which vascular, inflammatory/autoimmune, and fibrotic processes occur simultaneously and contribute to organ damage. Early recognition and treatment of symptoms and life-threatening complications are therefore crucial

for SSc patient clinical evolution (66). The capacity of FPRs, through the interaction with the uPA/uPAR system, to trigger the transformation of fibroblasts to myofibroblast and to coordinate proliferation and cell migration makes them a potential novel therapeutic target in the treatment of early SSc.

Disclosures

The authors have no financial conflicts of interest.

References

1. Katsumoto, T. R., M. L. Whitfield, and M. K. Connolly. 2011. The pathogenesis of systemic sclerosis. *Annu. Rev. Pathol.* 6: 509–537.
2. Manetti, M., S. Guiducci, and M. Matucci-Cerinic. 2011. The origin of the myofibroblast in fibroproliferative vasculopathy: does the endothelial cell steer the pathophysiology of systemic sclerosis? *Arthritis Rheum.* 63: 2164–2167.
3. Klingberg, F., B. Hinz, and E. S. White. 2013. The myofibroblast matrix: implications for tissue repair and fibrosis. *J. Pathol.* 229: 298–309.
4. Abraham, D. J., B. Eckes, V. Rajkumar, and T. Krieg. 2007. New developments in fibroblast and myofibroblast biology: implications for fibrosis and scleroderma. *Curr. Rheumatol. Rep.* 9: 136–143.
5. Gilbane, A. J., C. P. Denton, and A. M. Holmes. 2013. Scleroderma pathogenesis: a pivotal role for fibroblasts as effector cells. *Arthritis Res. Ther.* 15: 215.
6. Darby, I. A., and T. D. Hewitson. 2007. Fibroblast differentiation in wound healing and fibrosis. *Int. Rev. Cytol.* 257: 143–179.
7. Piera-Velazquez, S., Z. Li, and S. A. Jimenez. 2011. Role of endothelial-mesenchymal transition (EndoMT) in the pathogenesis of fibrotic disorders. *Am. J. Pathol.* 179: 1074–1080.
8. Jimenez, S. A. 2013. Role of endothelial to mesenchymal transition in the pathogenesis of the vascular alterations in systemic sclerosis. *ISRN Rheumatol.* 2013: 835948.
9. Rajkumar, V. S., K. Howell, K. Csiszar, C. P. Denton, C. M. Black, and D. J. Abraham. 2005. Shared expression of phenotypic markers in systemic sclerosis indicates a convergence of pericytes and fibroblasts to a myofibroblast lineage in fibrosis. *Arthritis Res. Ther.* 7: R1113–R1123.
10. Abraham, D. J., T. Krieg, J. Distler, and O. Distler. 2009. Overview of pathogenesis of systemic sclerosis. *Rheumatology* 48(Suppl. 3): iii3–iii7.
11. Le, Y., P. M. Murphy, and J. M. Wang. 2002. Formyl-peptide receptors revisited. *Trends Immunol.* 23: 541–548.
12. Ye, R. D., F. Boulay, J. M. Wang, C. Dahlgren, C. Gerard, M. Parmentier, C. N. Serhan, and P. M. Murphy. 2009. International Union of Basic and Clinical Pharmacology. LXXIII. Nomenclature for the formyl peptide receptor (FPR) family. *Pharmacol. Rev.* 61: 119–161.
13. Li, Y., and D. Ye. 2013. Molecular biology for formyl peptide receptors in human diseases. *J. Mol. Med.* 91: 781–789.
14. de Paulis, A., N. Prevete, I. Fiorentino, A. F. Walls, M. Curto, A. Petraroli, V. Castaldo, P. Ceppa, R. Fiocca, and G. Marone. 2004. Basophils infiltrate human gastric mucosa at sites of *Helicobacter pylori* infection, and exhibit chemotaxis in response to *H. pylori*-derived peptide Hp(2-20). *J. Immunol.* 172: 7734–7743.
15. Gao, J. L., A. Guillabert, J. Hu, Y. Le, E. Urizar, E. Seligman, K. J. Fang, X. Yuan, V. Imbault, D. Communi, et al. 2007. F2L, a peptide derived from heme-binding protein, chemoattracts mouse neutrophils by specifically activating Fpr2, the low-affinity *N*-formylpeptide receptor. *J. Immunol.* 178: 1450–1456.
16. de Paulis, A., N. Prevete, F. W. Rossi, F. Rivellese, F. Salerno, G. Delfino, B. Liccardo, E. Avilla, N. Montuori, M. Mascolo, et al. 2009. *Helicobacter pylori* Hp(2-20) promotes migration and proliferation of gastric epithelial cells by interacting with formyl peptide receptors in vitro and accelerates gastric mucosal healing in vivo. *J. Immunol.* 183: 3761–3769.
17. Prevete, N., F. A. Salzano, F. W. Rossi, F. Rivellese, M. Dellepiane, L. Guastini, R. Mora, G. Marone, A. Salami, and A. De Paulis. 2011. Role(s) of formyl-peptide receptors expressed in nasal epithelial cells. *J. Biol. Regul. Homeost. Agents* 25: 553–564.
18. Madsen, C. D., and N. Sidenius. 2008. The interaction between urokinase receptor and vitronectin in cell adhesion and signalling. *Eur. J. Cell Biol.* 87: 617–629.
19. Arciniegas, E., Y. C. Neves, and L. M. Carrillo. 2006. Potential role for insulin-like growth factor II and vitronectin in the endothelial-mesenchymal transition process. *Differentiation* 74: 277–292.
20. Ragno, P. 2006. The urokinase receptor: a ligand or a receptor? Story of a sociable molecule. *Cell. Mol. Life Sci.* 63: 1028–1037.
21. Montuori, N., V. Cosimato, L. Rinaldi, V. E. Rea, D. Alfano, and P. Ragno. 2013. uPAR regulates pericellular proteolysis through a mechanism involving integrins and fMLF-receptors. *Thromb. Haemost.* 109: 309–318.
22. Smith, H. W., and C. J. Marshall. 2010. Regulation of cell signalling by uPAR. *Nat. Rev. Mol. Cell Biol.* 11: 23–36.
23. Montuori, N., and P. Ragno. 2009. Multiple activities of a multifaceted receptor: roles of cleaved and soluble uPAR. *Front. Biosci. (Landmark Ed.)* 14: 2494–2503.
24. Preissner, K. T., and U. Reuning. 2011. Vitronectin in vascular context: facets of a multitalented matricellular protein. *Semin. Thromb. Hemost.* 37: 408–424.
25. López-Guisa, J. M., A. C. Rassa, X. Cai, S. J. Collins, and A. A. Eddy. 2011. Vitronectin accumulates in the interstitium but minimally impacts fibrogenesis in experimental chronic kidney disease. *Am. J. Physiol. Renal Physiol.* 300: F1244–F1254.
26. Montuori, N., M. V. Carriero, S. Salzano, G. Rossi, and P. Ragno. 2002. The cleavage of the urokinase receptor regulates its multiple functions. *J. Biol. Chem.* 277: 46932–46939.
27. Resnati, M., I. Pallavicini, J. M. Wang, J. Oppenheim, C. N. Serhan, M. Romano, and F. Blasi. 2002. The fibrinolytic receptor for urokinase activates the G protein-coupled chemotactic receptor FPRL1/LXA4R. *Proc. Natl. Acad. Sci. USA* 99: 1359–1364.
28. de Paulis, A., N. Montuori, N. Prevete, I. Fiorentino, F. W. Rossi, V. Visconte, G. Rossi, G. Marone, and P. Ragno. 2004. Urokinase induces basophil chemotaxis through a urokinase receptor epitope that is an endogenous ligand for formyl peptide receptor-like 1 and -like 2. *J. Immunol.* 173: 5739–5748.
29. Postiglione, L., N. Montuori, A. Riccio, G. Di Spigna, S. Salzano, G. Rossi, and P. Ragno. 2010. The plasminogen activator system in fibroblasts from systemic sclerosis. *Int. J. Immunopathol. Pharmacol.* 23: 891–900.
30. D'Alessio, S., G. Fibbi, M. Cinelli, S. Guiducci, A. Del Rosso, F. Margheri, S. Serratì, M. Pucci, B. Kahaleh, P. Fan, et al. 2004. Matrix metalloproteinase 12-dependent cleavage of urokinase receptor in systemic sclerosis microvascular endothelial cells results in impaired angiogenesis. *Arthritis Rheum.* 50: 3275–3285.
31. van den Hoogen, F., D. Khanna, J. Fransen, S. R. Johnson, M. Baron, A. Tyndall, M. Matucci-Cerinic, R. P. Naden, T. A. Medsger, Jr., P. E. Carreira, et al. 2013. 2013 classification criteria for systemic sclerosis: an American College of Rheumatology/European League against Rheumatism collaborative initiative. *Arthritis Rheum.* 65: 2737–2747.
32. LeRoy, E. C., C. Black, R. Fleischmajer, S. Jablonska, T. Krieg, T. A. Medsger, Jr., N. Rowell, and F. Wollheim. 1988. Scleroderma (systemic sclerosis): classification, subsets and pathogenesis. *J. Rheumatol.* 15: 202–205.
33. Manetti, M., S. Guiducci, E. Romano, I. Rosa, C. Ceccarelli, T. Mello, A. F. Milia, M. L. L. Conforti, L. Ibba-Manneschi, and M. Matucci-Cerinic. 2013. Differential expression of junctional adhesion molecules in different stages of systemic sclerosis. *Arthritis Rheum.* 65: 247–257.
34. Svensson, L., E. Redvall, C. Björn, J. Karlsson, A. M. Bergin, M. J. Rabiet, C. Dahlgren, and C. Wennerås. 2007. House dust mite allergen activates human eosinophils via formyl peptide receptor and formyl peptide receptor-like 1. *Eur. J. Immunol.* 37: 1966–1977.
35. de Paulis, A., N. Prevete, I. Fiorentino, F. W. Rossi, S. Staibano, N. Montuori, P. Ragno, A. Longobardi, B. Liccardo, A. Genovese, et al. 2006. Expression and functions of the vascular endothelial growth factors and their receptors in human basophils. *J. Immunol.* 177: 7322–7331.
36. Bocchino, M., S. Agnese, E. Fagone, S. Svegliati, D. Grieco, C. Vancheri, A. Gabrielli, A. Sanduzzi, and E. V. Avvedimento. 2010. Reactive oxygen species are required for maintenance and differentiation of primary lung fibroblasts in idiopathic pulmonary fibrosis. *PLoS One* 5: e14003. Available at: http://journals.plos.org/plosone/article?id=10.1371/journal.pone.0014003.
37. Snedecor, G. W., and W. G. Cochran. 1980. *Statistical methods*, 7th Ed. Iowa State University Press, Ames, IA.
38. Selleri, C., N. Montuori, P. Ricci, V. Visconte, M. V. Carriero, N. Sidenius, B. Serio, F. Blasi, B. Rotoli, G. Rossi, and P. Ragno. 2005. Involvement of the urokinase-type plasminogen activator receptor in hematopoietic stem cell mobilization. *Blood* 105: 2198–2205.
39. Viswanathan, A., R. G. Painter, N. A. Lanson, Jr., and G. Wang. 2007. Functional expression of *N*-formyl peptide receptors in human bone marrow-derived mesenchymal stem cells. *Stem Cells* 25: 1263–1269.
40. Chigaev, A., A. Waller, O. Amit, and L. A. Sklar. 2008. Gαs-coupled receptor signaling actively down-regulates $\alpha_4\beta_1$-integrin affinity: a possible mechanism for cell de-adhesion. *BMC Immunol.* 9: 26.
41. Huang, J., K. Chen, J. Chen, W. Gong, N. M. Dunlop, O. M. Howard, Y. Gao, X. W. Bian, and J. M. Wang. 2010. The G-protein-coupled formylpeptide receptor FPR confers a more invasive phenotype on human glioblastoma cells. *Br. J. Cancer* 102: 1052–1060.
42. Liu, S., S. W. Xu, K. Blumbach, M. Eastwood, C. P. Denton, B. Eckes, T. Krieg, D. J. Abraham, and A. Leask. 2010. Expression of integrin β_1 by fibroblasts is required for tissue repair in vivo. *J. Cell Sci.* 123: 3674–3682.
43. Shi-wen, X., K. Thompson, K. Khan, S. Liu, H. Murphy-Marshman, M. Baron, C. P. Denton, A. Leask, and D. J. Abraham. 2012. Focal adhesion kinase and reactive oxygen species contribute to the persistent fibrotic phenotype of lesional scleroderma fibroblasts. *Rheumatology* 51: 2146–2154.
44. Dooley, A., X. Shi-Wen, N. Aden, T. Tranah, N. Desai, C. P. Denton, D. J. Abraham, and R. Bruckdorfer. 2010. Modulation of collagen type I, fibronectin and dermal fibroblast function and activity, in systemic sclerosis by the antioxidant epigallocatechin-3-gallate. *Rheumatology* 49: 2024–2036.
45. Serratì, S., F. Margheri, A. Chillà, E. Neumann, U. Müller-Ladner, M. Benucci, G. Fibbi, and M. Del Rosso. 2011. Reduction of in vitro invasion and in vivo cartilage degradation in a SCID mouse model by loss of function of the fibrinolytic system of rheumatoid arthritis synovial fibroblasts. *Arthritis Rheum.* 63: 2584–2594.
46. Montuori, N., K. Bifulco, M. V. Carriero, C. La Penna, V. Visconte, D. Alfano, A. Pesapane, F. W. Rossi, S. Salzano, G. Rossi, and P. Ragno. 2011. The cross-talk between the urokinase receptor and fMLP receptors regulates the activity of the CXCR4 chemokine receptor. *Cell. Mol. Life Sci.* 68: 2453–2467.
47. Leask, A. 2012. Getting out of a sticky situation: targeting the myofibroblast in scleroderma. *Open Rheumatol. J.* 6: 163–169.
48. Asano, Y., H. Ihn, K. Yamane, M. Kubo, and K. Tamaki. 2004. Increased expression levels of integrin $\alpha_v\beta_5$ on scleroderma fibroblasts. *Am. J. Pathol.* 164: 1275–1292.
49. Gargiulo, L., I. Longanesi-Cattani, K. Bifulco, P. Franco, R. Raiola, P. Campiglia, P. Grieco, G. Peluso, M. P. Stoppelli, and M. V. Carriero. 2005. Cross-talk between fMLP and vitronectin receptors triggered by urokinase receptor-derived SRSRY peptide. *J. Biol. Chem.* 280: 25225–25232.

50. Gabrielli, A., S. Svegliati, G. Moroncini, and D. Amico. 2012. New insights into the role of oxidative stress in scleroderma fibrosis. *Open Rheumatol J* 6: 87–95.
51. Leoni, G., A. Alam, P. A. Neumann, J. D. Lambeth, G. Cheng, J. McCoy, R. S. Hilgarth, K. Kundu, N. Murthy, D. Kusters, et al. 2013. Annexin A1, formyl peptide receptor, and NOX1 orchestrate epithelial repair. *J. Clin. Invest.* 123: 443–454.
52. Gorrasi, A., A. Li Santi, G. Amodio, D. Alfano, P. Remondelli, N. Montuori, and P. Ragno. 2014. The urokinase receptor takes control of cell migration by recruiting integrins and FPR1 on the cell surface. *PLoS One* 9: e86352. Available at: http://journals.plos.org/plosone/article?id=10.1371/journal.pone.0086352.
53. Bifulco, K., G. Votta, V. Ingangi, G. Di Carluccio, D. Rea, S. Losito, N. Montuori, P. Ragno, M. P. Stoppelli, C. Arra, and M. V. Carriero. 2014. Urokinase receptor promotes ovarian cancer cell dissemination through its 84-95 sequence. *Oncotarget* 5: 4154–4169.
54. Migeotte, I., D. Communi, and M. Parmentier. 2006. Formyl peptide receptors: a promiscuous subfamily of G protein-coupled receptors controlling immune responses. *Cytokine Growth Factor Rev.* 17: 501–519.
55. Shi-Wen, X., E. A. Renzoni, L. Kennedy, S. Howat, Y. Chen, J. D. Pearson, G. Bou-Gharios, M. R. Dashwood, R. M. du Bois, C. M. Black, et al. 2007. Endogenous endothelin-1 signaling contributes to type I collagen and CCN2 overexpression in fibrotic fibroblasts. *Matrix Biol.* 26: 625–632.
56. Xu, S. W., S. Liu, M. Eastwood, S. Sonnylal, C. P. Denton, A. J. Abraham, and A. Leask. 2009. Rac inhibition reverses the phenotype of fibrotic fibroblasts. *PLoS One* 4: e7438. Available at: http://journals.plos.org/plosone/article?id=10.1371/journal.pone.0007438.
57. Bernstein, A. M., S. S. Twining, D. J. Warejcka, E. Tall, and S. K. Masur. 2007. Urokinase receptor cleavage: a crucial step in fibroblast-to-myofibroblast differentiation. *Mol. Biol. Cell* 18: 2716–2727.
58. Manetti, M., I. Rosa, A. F. Milia, S. Guiducci, P. Carmeliet, L. Ibba-Manneschi, and M. Matucci-Cerinic. 2014. Inactivation of urokinase-type plasminogen activator receptor (uPAR) gene induces dermal and pulmonary fibrosis and peripheral microvasculopathy in mice: a new model of experimental scleroderma? *Ann. Rheum. Dis.* 73: 1700–1709.
59. Wang, L., C. M. Ly, C. Y. Ko, E. E. Meyers, D. A. Lawrence, and A. M. Bernstein. 2012. uPA binding to PAI-1 induces corneal myofibroblast differentiation on vitronectin. *Invest. Ophthalmol. Vis. Sci.* 53: 4765–4775.
60. Asano, Y., H. Ihn, K. Yamane, M. Jinnin, Y. Mimura, and K. Tamaki. 2005. Increased expression of integrin $\alpha_v\beta_3$ contributes to the establishment of autocrine TGF-β signaling in scleroderma fibroblasts. *J. Immunol.* 175: 7708–7718.
61. Asano, Y., H. Ihn, K. Yamane, M. Jinnin, and K. Tamaki. 2006. Increased expression of integrin $\alpha_v\beta_5$ induces the myofibroblastic differentiation of dermal fibroblasts. *Am. J. Pathol.* 168: 499–510.
62. Silvestri, I., I. Longanesi Cattani, P. Franco, G. Pirozzi, G. Botti, M. P. Stoppelli, and M. V. Carriero. 2002. Engaged urokinase receptors enhance tumor breast cell migration and invasion by upregulating $\alpha_v\beta_5$ vitronectin receptor cell surface expression. *Int. J. Cancer* 102: 562–571.
63. Gabrielli, A., S. Svegliati, G. Moroncini, G. Pomponio, M. Santillo, and E. V. Avvedimento. 2008. Oxidative stress and the pathogenesis of scleroderma: the Murrell's hypothesis revisited. *Semin. Immunopathol.* 30: 329–337.
64. Menshikov, M., O. Plekhanova, H. Cai, K. Chalupsky, Y. Parfyonova, P. Bashtrikov, V. Tkachuk, and B. C. Berk. 2006. Urokinase plasminogen activator stimulates vascular smooth muscle cell proliferation via redox-dependent pathways. *Arterioscler. Thromb. Vasc. Biol.* 26: 801–807.
65. Barnes, T. C., M. E. Anderson, S. W. Edwards, and R. J. Moots. 2012. Neutrophil-derived reactive oxygen species in SSc. *Rheumatology* 51: 1166–1169.
66. Nihtyanova, S. I., V. H. Ong, and C. P. Denton. 2014. Current management strategies for systemic sclerosis. *Clin. Exp. Rheumatol.* 32(2 Suppl. 81)156–164.